Numerical modelling of stone columns in unsaturated silty sand

R. Imam & A.R. Fotowat
Department of civil and environmental engineering, Amirkabir University of Technology (Tehran polytechnic), Tehran, Iran

ABSTRACT: Many studies have used physical modelling, mathematical analyses and full-scale testing to understand and predict the behaviour of stone columns. Such studies have mainly considered stone columns in saturated or dry soils and have used conventional soil mechanics. However, in-situ soils are often in an unsaturated state and estimation of bearing capacity and settlement of stone columns using conventional methods often lead to conservative and costly designs. The present paper discusses numerical modelling of a series of physical model tests carried out on single stone columns installed in non-plastic, silty, fine sand at various degrees of saturation. Use of modified effective stress, soil strength and nonlinear soil stiffness obtained by considering soil suction developed in the unsaturated soil in numerical modelling of the model tests led to satisfactory match between observed and calculated load-deformation behaviour of the stone column. Results of the numerical modelling indicated that the ultimate bearing capacity obtained from the analysis of unsaturated soil is about 1.3 to 1.6 times higher than those of the nearly saturated and dry soils, respectively. Bulging in the upper portion of the stone column was also smaller in unsaturated soil conditions.

1 INTRODUCTION

The improvement of compressible soils by stone columns have become very popular in recent decades because of its substantial advantages. Stone columns are widely used to improve the bearing capacity of soft soils and decrease the time of consolidation of soils below distributed loads, embankments and structures due to their high strength, stiffness and permeability.

Several approaches have been adopted in the past to model and analyse stone columns. Some researchers used finite element analyses to evaluate the influence of stiffness of stone columns on their load-deformation behaviour (Balaam et al. 1977). A 2D/axisymmetric finite element parametric study has also been proposed to provide a prediction of settlements of granular columns by some other researchers (Sexton et al. 2014). However, the effects of characteristics of the surrounding unsaturated soils on the settlements and deformations have not been considered in these studies.

Effects of the state of the soil when it is in an intermediate condition in its saturation, between the two main limits of saturated and dry, has been the subject of many researches in the past decades. The Soil Water Characteristic Curve (SWCC) of an unsaturated soil determines important aspects of its engineering behaviour. This curve relates the volumetric water content (θ) or the degree of saturation (S) to the matric suction ($u_a - u_w$) of the soil, in which u_a and u_w are the air and pore water pressures, respectively. The residual degree of saturation, S_r, at which the degree of saturation decreases very slightly with increase in matric suction and the suction at air-entry value, $(u_a - u_w)_{AEV}$ at which air just starts to enter the soil following its saturation, are the main features that can be determined using this curve.

The bearing capacity of shallow foundations is significantly influenced by matric or capillary suction of an unsaturated soil and there is growing evidence confirming this conclusion (Rojas et al. 2007). Mohamed and Vanapalli (2006) showed that the bearing capacity of a square footing placed on coarse-grained soils is approximately 5 to 7 times higher than that on fully saturated soil. Lins et al. (2009) investigated the influence of matric suction on the bearing capacity of strip footings.

In the current study, results of numerical modelling of a single stone column fully penetrated in an unsaturated, non-plastic, silty, fine sand are presented. Results obtained using two modelling approaches are compared with data obtained from model tests. The study continues with an assessment of the influence of matric suction on the lateral expansion of the stone column and settlement of the surrounding soil and evaluates these effects when degree of saturation of the soil and properties of the stone column vary.

2 REFERENCE CASE

The reference case used for verification of the numerical modelling consists of a single stone column installed in an unsaturated Firoozkooh #101 silty sand loaded by a circular rigid footing (Vaseghi Maghvan et al. 2017). The sand was placed in 9 layers 5 cm thick each and prepared at specified degrees of saturation in a rectangular test box having 45 cm height, 70 cm length and 50 cm width. The box walls consisted of plexiglass on two opposite sides, and metal sheets on the other two sides, with stiffeners to prevent their lateral deformations. Installation of the stone column was carried out by penetrating a 5 cm inside diameter plastic tube in the soil, removing the soil from inside the tube and placing and compacting the stone column material in the hole. A vertical displacement at a rate of 1 mm/min was applied to the footing until a maximum displacement of 75 mm was reached. The footing diameter, B, was 10 cm and the column diameter, D_s, was 5.6 cm at the end of the installation. Final column length was 45 cm.

Strength parameters of the soil and column materials were obtained using simple shear testing at 0% saturation and are shown in Table 1. Maximum and minimum void ratios were 0.9 and 0.68, respectively for the soil and 0.98 and 0.67, respectively for the column. After placement, the soil relative density was determined to be 40% corresponding to a void ratio of 0.811 and a unit weight of 14.36 KN/m^3. Relative density of the column material after placement was 60%, corresponding to a unit weight of 15 KN/m^3.

Table 1. Soil and column properties obtained from direct shear tests (Vaseghi Maghvan et al. 2017).

	Soil	Stone column
Effective Cohesion (kPa)	3.5	0
Effective friction angle	31.5	39.5

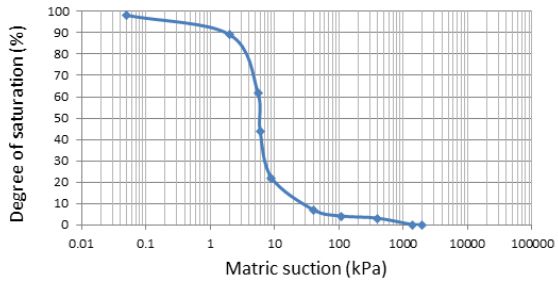

Figure 1. Soil-water characteristic curve of the soil.

The SWCC of the soil obtained experimentally using the filter paper method is shown in Figure 1 (Vaseghi Magvan et al. 2017). The air-entry and residual suctions were 3.9 kPa and 9.1 kPa, respectively. The residual (S_r) and the air-entry (S_e) saturations were determined to be 6% and 92%, respectively.

3 NUMERICAL AND MATERIAL MODELING

3.1 *Basic assumptions and theoretical background*

Finite element load-deformation analyses were performed using soil and stone column dimensions and properties the same as those used and obtained from test results as described before.

Since boundaries of the soil have sufficient distance from the column, about 10D, they are expected to have no effect on the deformations and stresses of the column, hence, a 2D axisymmetric modelling was used instead of a 3D modelling. The soil profile was assumed to consist of one homogeneous layer with a constant degree of saturation used for each analysis. The stone column was assumed to consist of an elastic-perfectly plastic material with a Mohr-Coulomb yield criterion. A small, non-zero cohesion (c_c = 0.01 kPa) was used for the column material to avoid numerical problems. It is very difficult to actually measure the dilatancy angle of the column material, especially in the field (Herle et al. 2008). Therefore, this parameter is usually taken as a reasonable estimation based on other in-situ properties (Castro 2014). Typical values of dilatancy, $\psi = 5^0$ and elastic modulus of E_{rc} = 45 MPa were chosen for the column material. Poisson ratios of the column and soil were estimated to be 0.25 and 0.3, respectively. A constant degree of saturation was used for all the soil and no ground water level was modelled.

The mesh property is generated locally and globally using triangular and quadratic or mixed elements to ensure a good quality of the numerical analysis. The mesh generation will be completed as meshing will be compatible across different regions or material properties or boundary conditions. As the column and the surrounding soil are tightly interlocked, no interface is defined between them. The circular foundation is assumed to be rigid due to the very stiff plate, producing uniform settlement. Mesh sensitivity studies were performed to ensure that the mesh was fine enough to give reliable results for the models used. The finite element model is shown in Figure 2.

All numerical simulations were performed using axisymmetric modelling with the assumption of drained condition for all the process. Consequently, all the responses were studied using effective stress analyses. Modelling was carried out in two stages: an initial condition to determine in-situ stresses for the soil with horizontal surface and the second stage, for the determination of the load deformation behaviour, following installation of the stone column and the foundation and application of the loading. Strain-control loading with an ultimate settlement of 75 mm for evaluating stress-displacement and lateral expansion behaviour and a uniform 20 kPa loading for evaluating the effect of the ratio H/B on settlement of the stone column. Roller boundaries for the

sides and boundaries fixed both horizontally and vertically were used at the bottom of the finite element model.

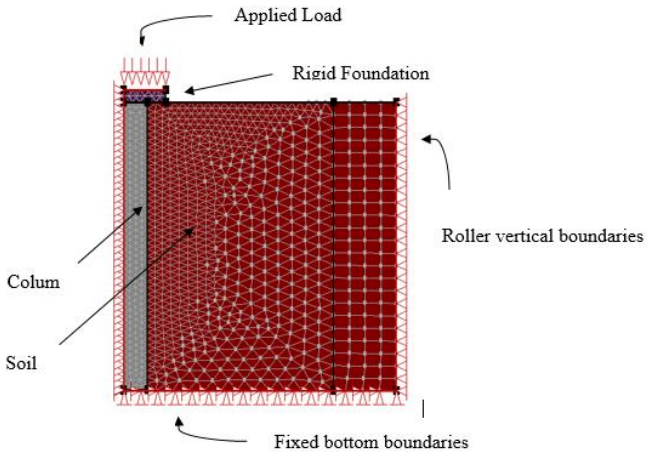

Figure 2. The 2D finite element model used.

3.2 *Modelling Unsaturated Soil Conditions*

Two different approaches were used in modelling the behaviour of soils improved by stone column. First one involved using the nonlinear elastic model with soil stresses and properties modified by matric suction in the unsaturated soil and second one was based on the assumption of a linear elastic behaviour and the Mohr-Coulomb yielding/failure criterion in which the shear strength and deformation parameters are modified due to the soil matric suction. Modifications of the strength and deformation properties and soil stresses are described in the following paragraphs.The following relationship was proposed by Fredlund et al. (1978) for calculating the shear strength of an unsaturated soil:

$$\tau_{unsat} = c' + (u_a - u_w)\tan\varphi^b + (\sigma - u_a)\tan\varphi' \quad (1)$$

where, τ_{unsat} is the shear strength of the unsaturated soil; c' and φ' are the effective shear strength parameters and φ^b is an angle indicating the rate of increase in shear strength with the matric suction (u_a – to account for the increase in shear strength due to unsaturated soil condition by combining this increase with the effective cohesion to yield a modified effective cohesion, c as proposed in the following relationship by Vanapalli et al. (1996):

$$c = c' + (u_a - u_w)\tan\varphi' \frac{(\theta - \theta_r)}{(\theta_s - \theta_r)} \quad (2)$$

where, θ, θ_s and θ_r are the current, saturated and residual water contents, respectively. In using the Mohr-Coulomb failure criterion in the current study, soil cohesion was modified manually for each analysis using the above equation.

Matric suctions corresponding to the water content or degree of saturation of the soil were obtained using the SWCC (Fig. 1). Based on Bishop (1959), the effect of matric suction on the effective stresses were determined as the product of the matric suction and the effective stress parameter, χ, which was calculated using Equation 3, (Russell & Khalili 2006). Parameters used in the analyses are shown in Table 2.

$$\chi = \begin{cases} 1 & for \quad \dfrac{(u_a - u_w)}{(u_a - u_w)_b} < 1 \\ \left(\dfrac{(u_a - u_w)}{(u_a - u_w)_b}\right)^{-0.55} & for \quad 1 < \dfrac{(u_a - u_w)}{(u_a - u_w)_b} < 25 \\ 25^{0.45}\left(\dfrac{(u_a - u_w)}{(u_a - u_w)_b}\right)^{-1} & for \quad \dfrac{(u_a - u_w)}{(u_a - u_w)_b} > 25 \end{cases} \quad (3)$$

Table 2. Modified soil cohesion and negative PWP of the soil for various degrees of saturation.

Degree of saturation (%)	Modified cohesion (kPa)	$u_a - u_w$ (m)	χ	Modified PWP (m)
4	7.78	-321	0.011	-3.53
16	4.54	-16	0.5	-8
30	4.56	-7	0.7	-4.9
60	5.43	-5.5	0.8	-4.4
90	5.14	-3	0.99	-2.97

Modified PWP in Table 2 is obtained by multiplying χ given by Equation 3 and the matric suction, $u_a - u_w$. Modulus of elasticity of the unsaturated sand can be determined using Equation 4 proposed by Oh et al. (2009).

$$E_{unsat} = E_{sat}[1 + \alpha \frac{(u_a - u_w)}{P_a / 101.3} S^{\beta}] \quad (4)$$

where, E_{unsat} and E_{sat} are the moduli of elasticity under unsaturated and saturated conditions, respectively; P_a is the atmospheric pressure (101.3 kPa); u_w is the pore water pressure and ($\sigma - u_a$) is the net normal stress. It is possible, S is the degree of saturation. Fitting parameters, α and β of 0.01 and 2, respectively were used based on past experience (Adem & Vanapalli 2015).

3.3 *Hyperbolic and elastoplastic models for the soil*

As a first approach, the soil was assumed as a nonlinear material behaving as predicted by the hyperbolic Duncan and Chang model. In this model, the soil stiffness is a function of the confining stress (Duncan et al. 1980) and is calculated using the initial soil modulus E_i, the soil friction angle and cohesion and the parameter R_f, which is the ratio between the asymptote to the hyperbolic curve and the maximum shear strength. The initial soil modulus is calculated using Equation 3, where n and K_L are modulus parameters. A value of 0.7 was chosen for the R_f as suggested by Duncan et al. (1980) for granular soils and n and K_L were determined using results of three consolidated-drained triaxial tests on Firoozkooh sand at a relative density of 40% used in the reference case (Figure 3).

Table 3 presents the initial tangent moduli for the confining pressures used in these tests. Based on these results, modulus parameters, n and K_L, of 0.23 and 265 were obtained, respectively, using Equation 3.

$$E_i = K_L P_a \left(\frac{\sigma_3}{P_a}\right)^n \quad (5)$$

In Equation 5, σ_3 and P_a are the confining and atmospheric pressures, respectively and n is an exponent for defining the effect of the confining pressure on the initial modulus. The modified moduli of elasticity for the soil with hyperbolic behaviour are shown in Table 4. Analyses were also carried out in which the soil was considered as an elastic-perfectly plastic material following the Mohr-Coulomb yielding/failure criterion. A saturated elastic modulus of E_{sat} = 15 MPa and strength parameters the same as those used in the hyperbolic model were adopted. The unsaturated moduli of elasticity for this model obtained from Equation 3 are shown in Table 5.

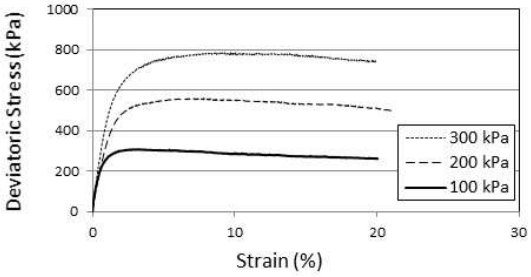

Figure 3. Deviatoric stress- strain for Firoozkooh sand.

Table 3. Initial tangent moduli for various confining pressures.

Confining pressure (kPa)	E_i (kPa)
100	26700
200	31320
300	34380

Table 4. Modified moduli of elasticity for hyperbolic model.

S_r (%)	Modified E_i (kPa)			n	K_L
	σ_3=100 kPa	σ_3=200 kPa	σ_3=300 kPa		
4	26837	31480	34556	0.226	266
16	26809	31448	34520	0.228	267
30	26868	31517	34596	0.224	267
60	27228	31940	35060	0.222	268
90	27348	32081	35215	0.221	269

Table 5. Modified elastic moduli for the elastic-plastic model.

Degree of saturation (%)	Modified E_{unsat} (kPa)
4	15077
16	15061
30	15094
60	15297
90	15364

4 RESULTS AND DISCUSSION

4.1 *Degree of saturation*

The first set of analyses involved the examination of the influence of degree of saturation on the stress-displacement behaviour of the stone column. Comparison of model predictions and experimental results obtained by Vaseghi Maghvan et al. (2017) for degrees of saturation of S_r = 0%, 4%, 16%, 30%, 60% and 90% are shown in Figure 4 to 9. When the hyperbolic model is used, modelled and measured results are closely compared to the elastic-plastic Mohr-Coulomb (MC) model. The MC model results are closer to measured behaviour for S_r = 4%, 16% and 30%, in which two slopes in the stress-displacement curve, similar to the experimental and hyperbolic results, are observed. However, for S_r = 0%, 60% and 90%, it exhibits a considerably smaller slope for displacements less than 20 mm. This may be attributed to the development of yield zones in the soils with degrees of saturation that result in lower strengths, as will be seen later. As a result, softer stress-strain responses are predicted for these cases.

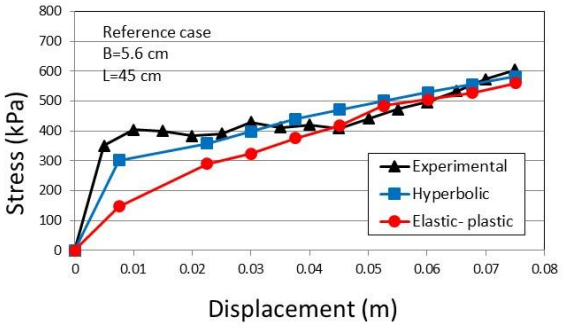

Figure 4. Stress- displacement for S_r = 0%.

Figures 10 and 11 show bearing pressures corresponding to the maximum applied displacement of 75 mm and a displacement of 15 mm, which may be considered as approximately corresponding to the bearing capacity of the stone column, respectively. The results exhibit a sharp increase in strength from

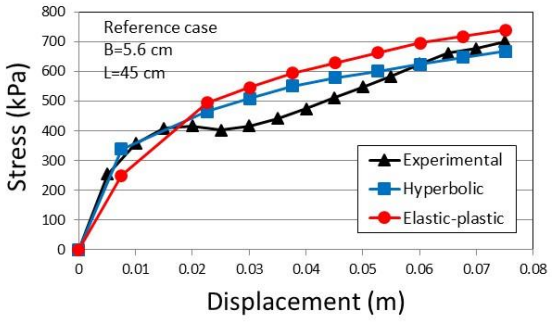

Figure 5. Stress- displacement for S_r = 4%.

S_r = 0% to S_r = 16%, followed by decrease with a similar slope up to about S_r = 35 or 40%. The strength then decreases at a smaller rate, until it reaches to minimum at S_r = 90%. This indicates that

the behaviour is more sensitive to changes in soil moisture in the saturation interval of 0% to 40% compared to saturations greater than 40%.

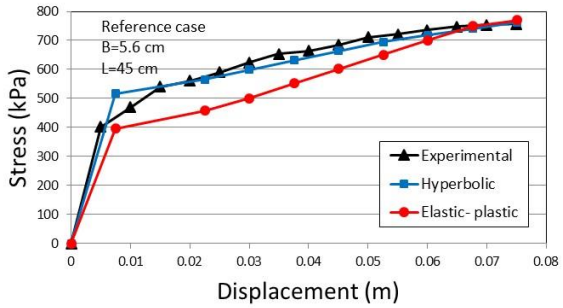

Figure 6. Stress- displacement for S_r = 16%.

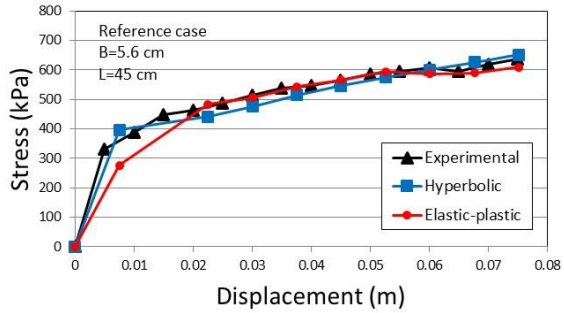

Figure 7. Stress- displacement for S_r = 30%.

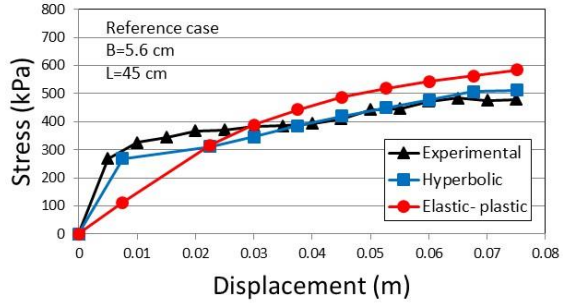

Figure 8. Stress- displacement for S_r = 60%.

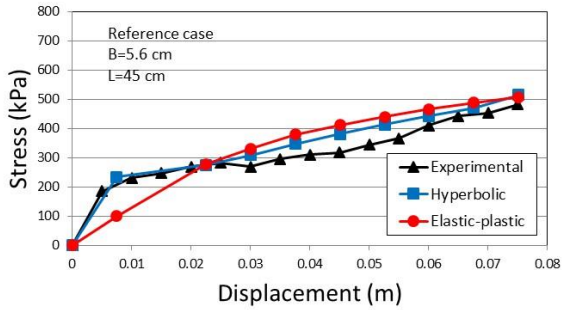

Figure 9. Stress- displacement for S_r = 90%.

Results also indicate that, in general, decrease in the degree of saturation and hence, increase in the matric suction improves soil strength and results in stiffer stress-displacement behaviour compared to the near-saturated condition. For each displacement, the corresponding bearing stress is the highest for the soil with S_r=16% and lowest for the case with S_r=90% (nearly saturated condition). These results are consistent with the variation of shear strengths with degree of saturation obtained from direct shear tests on the sand used in the reference model tests reported by Imam et al. (2017), in which they obtained the highest and lowest shear strengths for S_r=16% and S_r=90%, respectively.

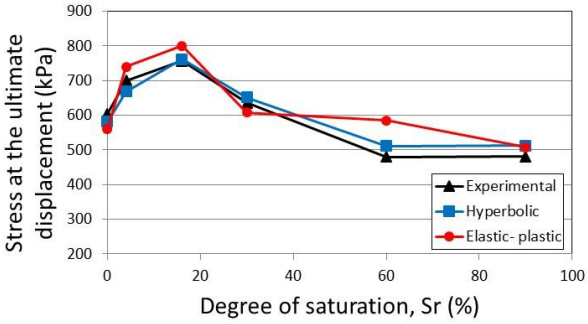

Figure 10. Stress at displacement of 75 mm versus different degrees of saturation.

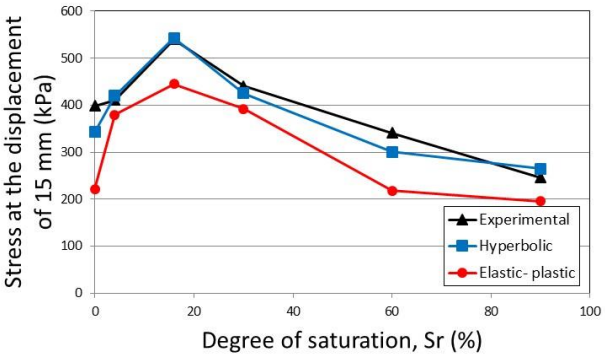

Figure 11. Stress at displacement of 15 mm versus different degrees of saturation.

4.2 *Lateral expansion*

Figure 12 shows lateral deformations obtained from numerical modelling for the cases with various degrees of saturation. It may be noticed that increase in soil strength and stiffness result in higher lateral confinement of the stone column and decrease in lateral expansion of the column. Bulging occurs near the upper part of the column due to the smaller confining stresses, as expected.

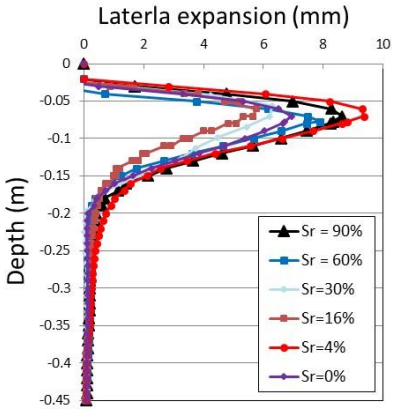

Figure 12. Lateral expansion with depth in different saturations for elastic- plastic model.

4.3 *Column length*

To study the influence of column length (H) on the stress-displacement behaviour of the stone column, length of the column was varied from 45 cm to 60 cm, 80 cm and 100 cm. For each column length, the soil layer thickness was assumed to be the same as the column length such that the column continues to be end-bearing. When *H*/*B* (*B* is footing width while column diameter is constant) decreases, the columns are better confined laterally, if they are not near the footing edges (Castro 2014). A 20 kPa load was applied on the footing at different degrees of saturation. Figure 13 shows that the settlement at the end of the loading increases with *H*/*B*, likely due to decrease in column confinement, and settlements are the smallest for S_r=16% and largest for S_r=4% and 90%.

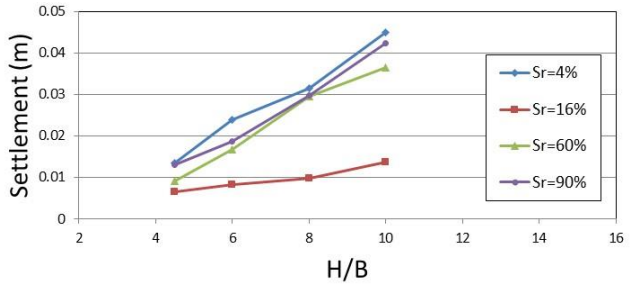

Figure 13. Variation of settlement with *H*/*B*

5 CONCLUSIONS

Results of the current numerical modelling indicate that the bearing capacity and bulging of the model stone column in silty sand is significantly influenced by the degree of saturation. The ultimate bearing capacity for unsaturated analyses was found to be 1.3 to 1.6 times higher in comparison to the nearly saturated and dry cases, respectively. It should be noted that the positive influence of the soil being partially saturated on bearing capacity of the stone column is less than on shallow foundations. For strip footings, the ratio of the maximum bearing capacity for unsaturated cases to fully saturated and dry cases are reported to be in the order of 4 and 2 to 2.5, respectively (Lins et al. 2009). Lateral expansion and bulging of the column showed a trend consistent with the changes in strength and stiffness of the soil with the degree of saturation.

Column settlement showed increment in the ratio of *H*/*B* for each degree of saturation. As expected, minimum and maximum settlements occurred at S_r=16%, and S_r=4% or 90%, respectively. At S_r=16%, the sensitivity to changes in the *H*/*B* ratio is also smaller compared to the other values of S_r.

The current study indicates that realistic prediction of the effects of degree of saturation on the behaviour of stone columns may be obtained if a proper SWCC and variations of soil properties with degree of saturation are used in numerical modelling.

6 REFERENCES

Adem, H.H. & Vanapalli, S.K. 2015. Prediction of the modulus of elasticity of compacted unsaturated expansive soils. *International Journal of Geotechnical Engineering* 9(2): 163-175.

Balaam, N., Brown, P. & Poulos, H. 1977. Settlement analysis of soft clays reinforced with granular piles. *The 5th Southeast Asian Conference on Soil Engineering*, Bangkok, Thailand.

Castro, J. 2014. Numerical modelling of stone columns beneath a rigid footing. *Computers and Geotechnics* 60: 77-87.

Duncan, J., Wong, K. S., & Mabry, P. (1980). Strength, stress-strain and bulk modulus parameters for finite element analyses of stresses and movements in soil masses *Geotechnical engineering*: University of California.

Fredlund, D.G., Morgenstem, N.R. & Widger, R.A. 1978. The shear strength of unsaturated soils. *Canadian Geotechnical Journal* 15(3): 313-321.

Herle, I., Wehr, J. & Arnold, M. 2008. Soil improvement with vibrated stone columns: influence of pressure level and relative density on friction angle. *The Proceedings of the 2nd International Conference on the Geotechnics of Soft Soils*, Glasgow: 235-240.

Imam, R., Vaseghi Maghvan, S. & Saaly, M. 2017. Laboratory Effects of hydraulic balance time on the shear strength of an unsaturated granular soil at various densities. *Proceedings of the 70th Canadian Geotechnical Conference*, Ottawa, Canada.

Lins, Y., Schanz, T. & Vanapalli, S. 2009. Bearing capacity and settlement behavior of a strip footing on an unsaturated coarse-grained soil. *The Proc., 4th Asia-Pacific Conf. on Unsaturated Soils.*

Mohamed, F. & Vanapalli, S. 2006. Laboratory investigations for the measurement of the bearing capacity of an unsaturated coarse-grained soil. *The Proceedings of the 59th Canadian Geotechnical Conference*, Vancouver, BC.

Oh, W. T., Vanapalli, S. K., & Puppala, A. J. (2009). Semi-empirical model for the prediction of modulus of elasticity for unsaturated soils. *Canadian Geotechnical Journal, 46*(8), 903-914.

Rojas, J.C., Salinas, L.M. & Sejas, C. 2007. Plate-load tests on an unsaturated lean clay. *Experimental unsaturated soil mechanics* Springer: 445-452.

Russell, A.R. & Khalili, N. 2006. On the problem of cavity expansion in unsaturated soils. *Computational Mechanics* 37(4): 311-330.

Sexton, B.G., McCabe, B.A. & Castro, J. 2014. Appraising stone column settlement prediction methods using finite element analyses. *Acta Geotechnica* 9(6): 993-1011.

Vanapalli, S., Fredlund, D., Pufahl, D. & Clifton, A. 1996. Model for the prediction of shear strength with respect to soil suction. *Canadian Geotechnical Journal* 33(3): 379-392.

Vaseghi Maghvan, S., Moazzami, A. & Imam, R. 2017. Laboratory model testing of stone columns in unsaturated silty sand. *Proceedings of the 70th Canadian Geotechnical Conference,* Ottawa, Canada.